Supporting Information

Fe-MIL Tuned and Binded by $Bi_4O_5Br_2$ for Boosting Photocatalytic Reduction of CO_2 to CH_4 under Simulated Sunlight

Xiaoli Li[a,b], Yuan Tang[a,b], Yue Jiang[a,b],Manman Mu[a,b*], Xiaohong Yin[a,b,c*]

a School of Chemistry and Chemical Engineering, Tianjin University of Technology, Tianjin 300384, PR China

b Tianjin Key Laboratory of Organic Solar Cells and Photochemical Conversion, Tianjin 300384, PR China

c College of Chemical Engineering and Materials Science, Tianjin University of Science &Technology, Tianjin 300457, PR China

Corresponding author:

Name: Xiaohong Yin E-mail: yinxiaohong@tjut.edu.cn Phone:13820315937

Address: Tianjin University of Technology, Tianjin 300384, PR China

Name: Manman Mu E-mail: mumanman@tju.edu.cn Phone:13920825181

Address:Tianjin University of Technology, Tianjin 300384, PR China

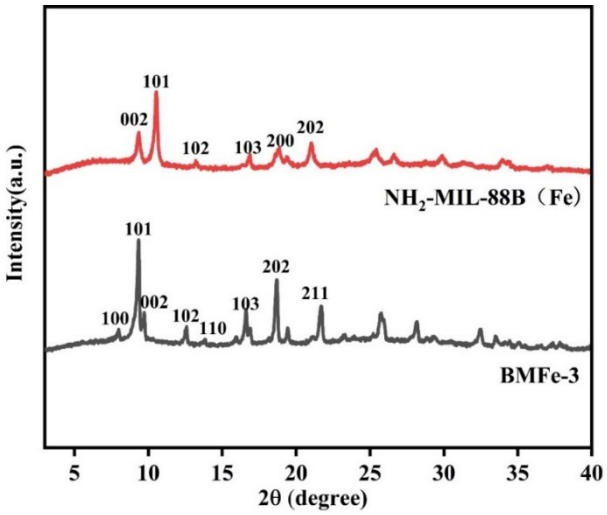

Fig. S1. XRD patterns of NH_2-MIL-88B(Fe) and BMFe-3.

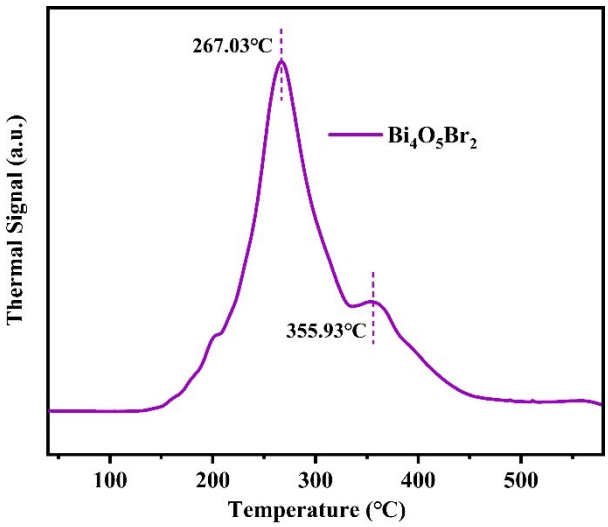

Fig. S2. NH_3-TPD analysis of $Bi_4O_5Br_2$

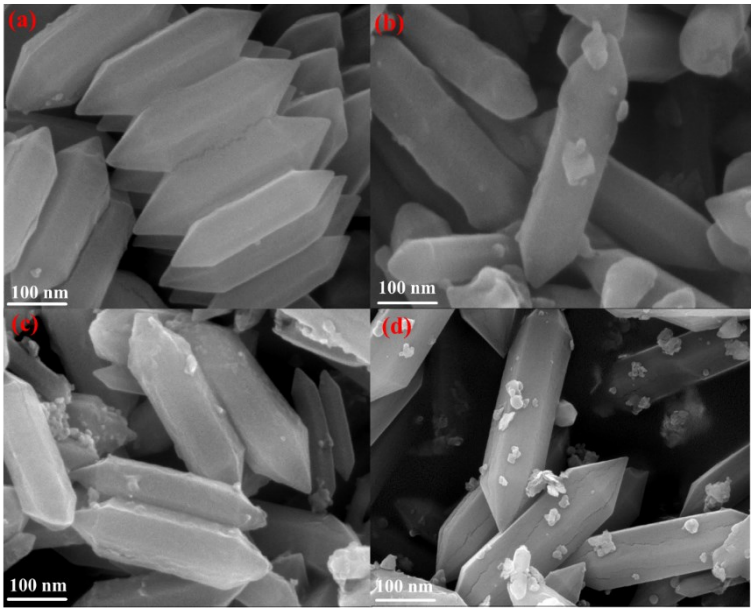

Fig. S3. SEM images of (a) BMFe-3 (b) BMFe-4(c) BMFe-5 (d) BMFe-6

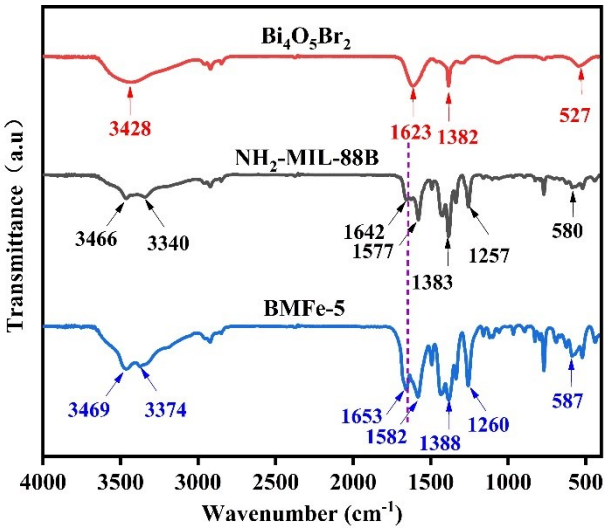

Fig. S4. FT-IR spectra of $Bi_4O_5Br_2$, NH_2-MIL-88B(Fe) and BMFe-5.

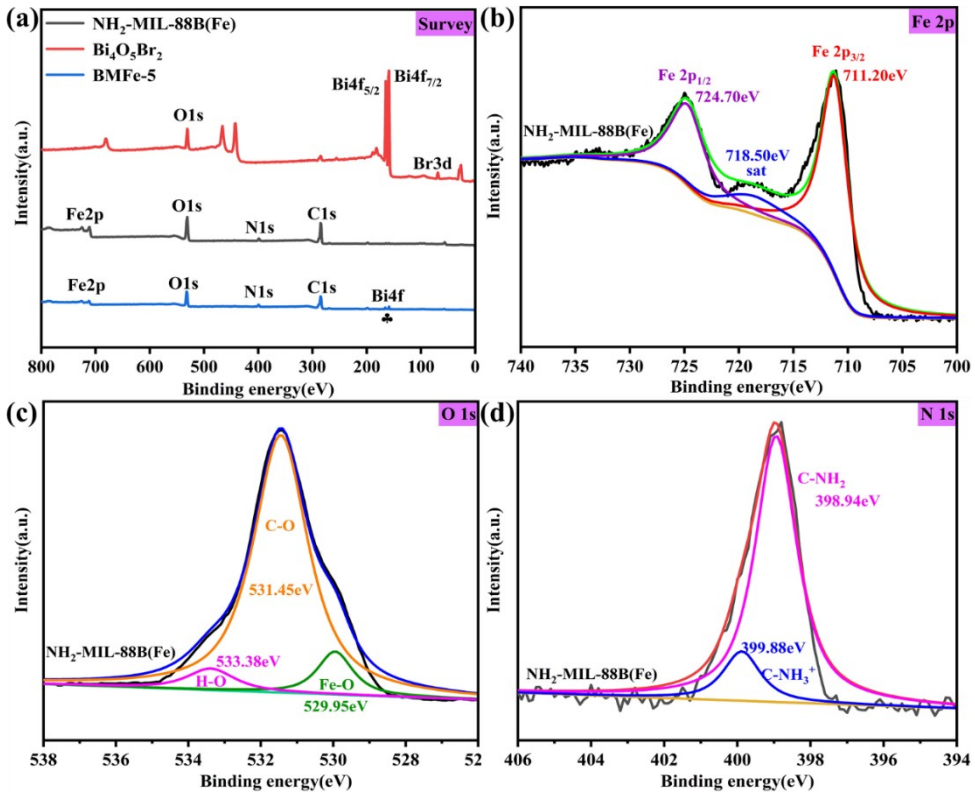

Fig. S5. XPS spectra: (a) Survey scan of NH_2-MIL-88B(Fe), $Bi_4O_5Br_2$ and BMFe-5, (b) Fe 2p, (c) O 1s and (d) N 1s of NH_2-MIL-88B(Fe).

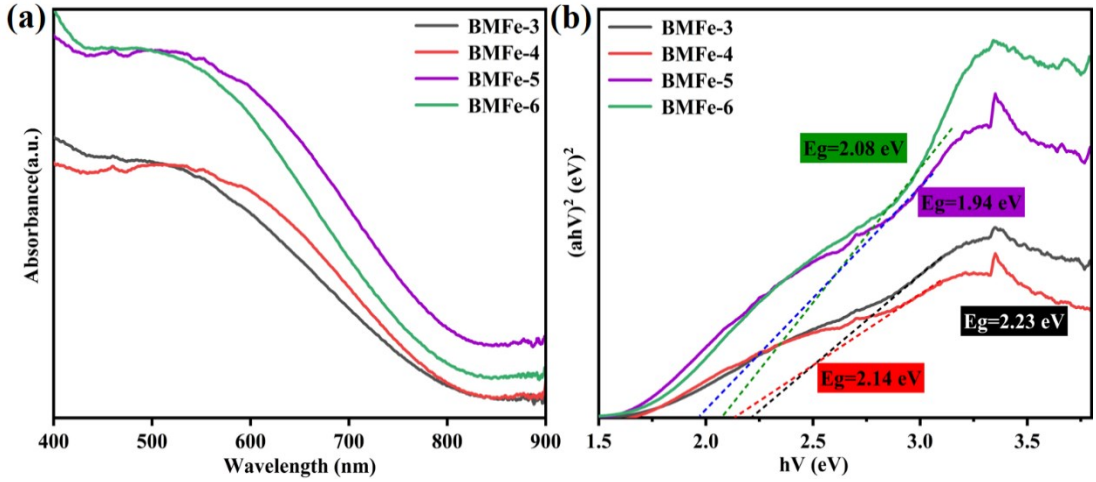

Fig. S6. (a) The UV–vis DRS and (b) the plot of $(\alpha hv)^2$ *vs* photo energy (hv) of BMFe-X (X=3, 4, 5, 6).

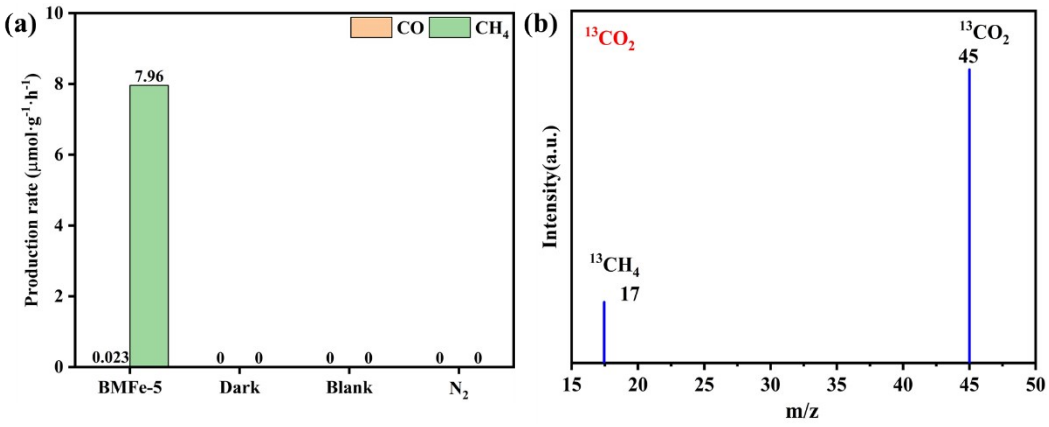

Fig. S7. (a) The control experiment of BMFe-5 under different reaction condition, (b) GC-MS analysis for the control experiment of $^{13}CO_2$

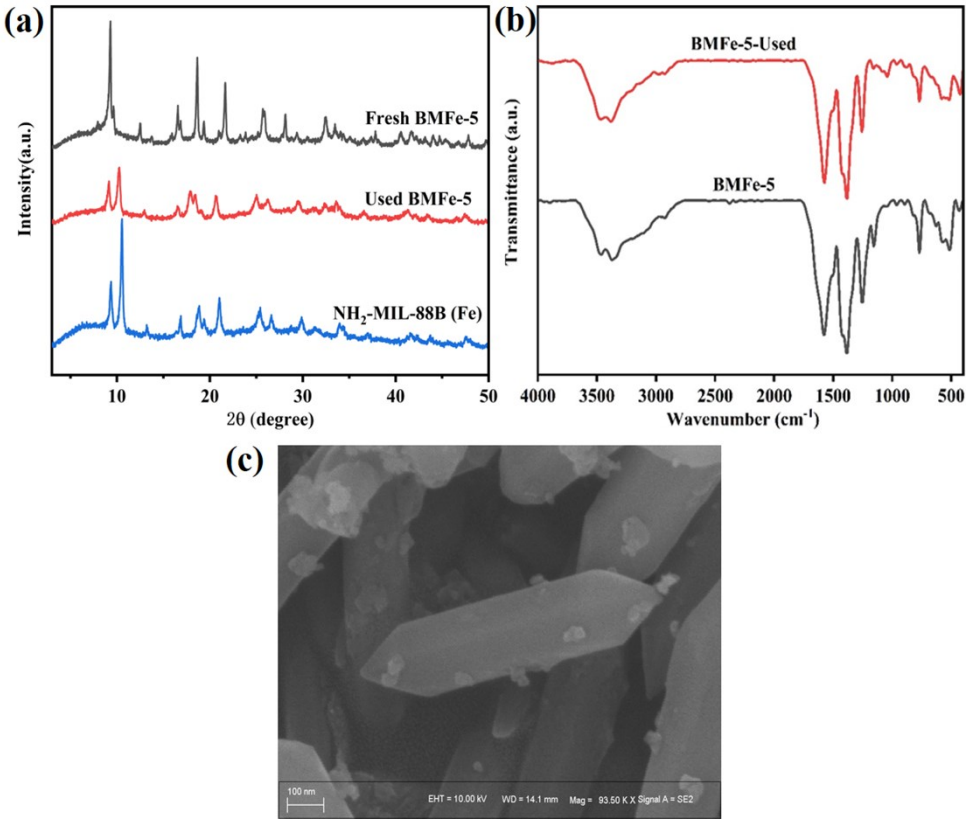

Fig. S8. (a) XRD, (b) FTIR patterns and (c) SEM image of BMFe-5 after four recycling tests

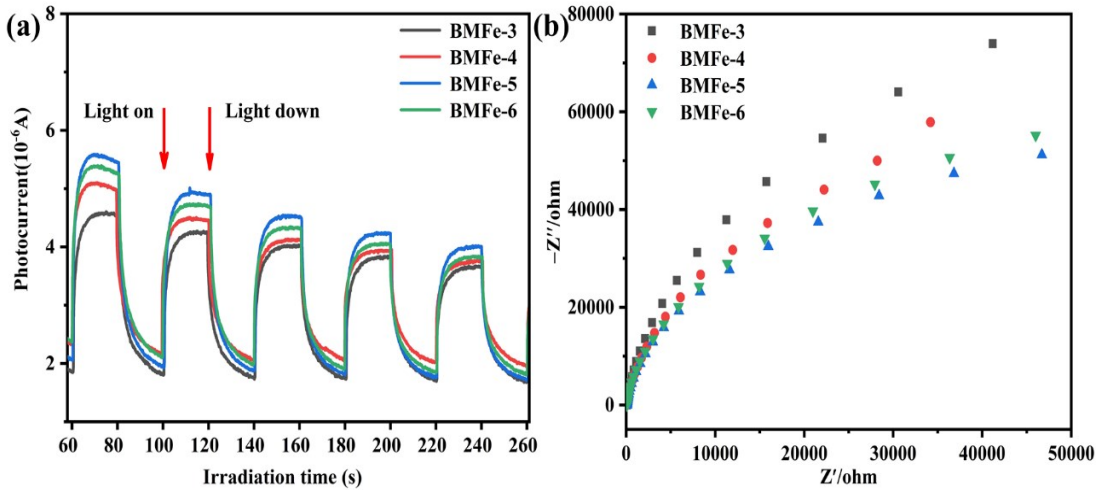

Fig. S9. (a) transient photocurrent responses and (b) EIS Nyquist plots of BMFe-X (X=3, 4, 5, 6).

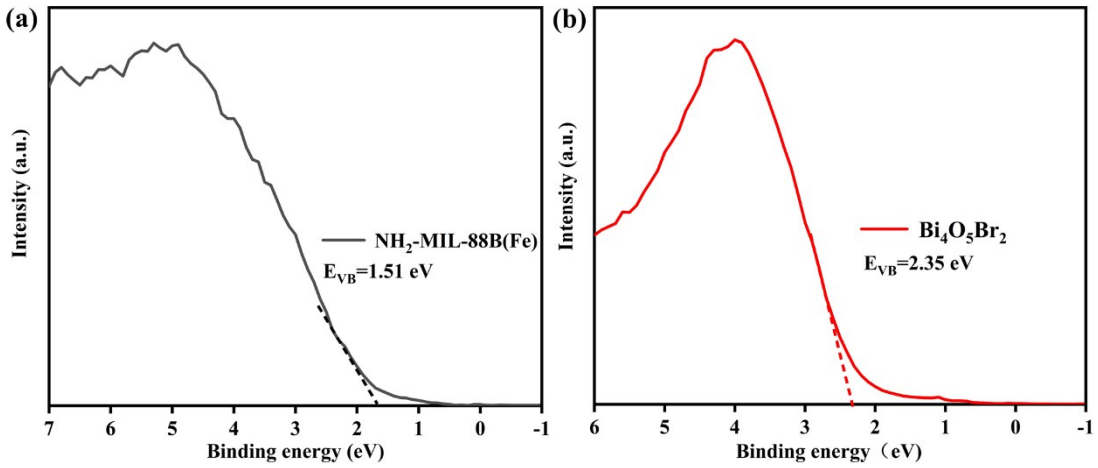

Fig. S10. The XPS valence band spectrum of (a) NH_2-MIL-88B(Fe) and (b) $Bi_4O_5Br_2$.

Table S1. The content of $Bi_4O_5Br_2$ in BMFe-X from ICP-MS test

Samples	The content of $Bi_4O_5Br_2$ (wt%)
BMFe-1	0.04
BMFe-2	0.06
BMFe-3	0.07
BMFe-4	0.40
BMFe-5	3.28
BMFe-6	8.93

Table S2. The textural properties of the samples

Samples	S_{BET} (m^2/g)	Total Pore Volume (cm^3/g)	Pore Size (nm)
NH_2-MIL-88(Fe)	72.39	0.127	7.01
$Bi_4O_5Br_2$	148.72	0.358	9.63
BMFe-5	21.15	0.052	9.82

Table S3 Comparisons of the amount of CO and CH_4 produced over different photocatalyst

Photocatalyst	The amount of CO ($\mu mol \cdot g^{-1} \cdot h^{-1}$)	The amount of CH_4 ($\mu mol \cdot g^{-1} \cdot h^{-1}$)	References
This work	**0.023**	**7.96**	**--**
CdS/ZIF-8	32.13	--	S1
UiO-66/CNNS	9.90	--	S2
Ni_3HITP_2/ rGO	12.82	--	S3
Co-MOF/g-C_3N_4	6.82	4.22	S4
Fe^{3+}-doped TiO_2	--	0.23	S5
Hollow $Bi_4O_5Br_2$	3.16	0.5	S6
Ultrathin $Bi_4O_5Br_2$	31.56	--	S7
Bi_2WO_6-OV/BiOI	--	2.29	S8
TiO_2/NH_2-MIL-125(Ti)	--	1.18	S9
$CsPbBr_3$QDs/UiO-66(NH_2)	8.21	0.26	S10

Table S4. The formation rates of CH_4 and CO, and selectivity of CH_4

Photocatalyst	Formation rate of CH_4 ($\mu mol \cdot g^{-1} \cdot h^{-1}$)	Formation rate of CO ($\mu mol \cdot g^{-1} \cdot h^{-1}$)	Selectivity of CH_4 [a]
NH_2-MIL-88(Fe)	0.05	0.02	71.43%
$Bi_4O_5Br_2$	0.42	0.471	47.19%
BMFe-3	4.21	0.013	99.62%
BMFe-4	6.38	0.021	99.79%
BMFe-5	7.96	0.023	99.74%
BMFe-6	7.51	0.018	99.76%

[a] Selectivity of CH_4 = (formation rate of CH_4)/ (formation rate of CH_4 + formation rate of CO).

Table S5 The Band gap (Eg), conduction band (E_{CB}), valence band (E_{VB}) and XPS valence band of NH_2-MIL-88B(Fe) and $Bi_4O_5Br_2$.

Samples	**E_g (eV)**	**E_{CB} (V)**	**E_{VB} (V)**	**$E_{VB\text{-}XPS}$ (eV)**
$Bi_4O_5Br_2$	2.68	-0.28	2.40	2.35
NH_2-MIL-88B(Fe)	1.86	-0.34	1.52	1.51

References

S1 Y. Liu, L. Deng, J. Sheng, F. Tang, K. Zeng, L. Wang, K. Liang, H. Hu, Y-N. Liu, *Applied Surface Science.,* 2019, 498, 143899.

S2 L. Shi, T. Wang, H. Zhang, K. Chang, J. Ye, *Adv. Funct. Mater.,* 2015, 25, 5360–5367.

S3 Q. Mu, W. Zhu, X. Li, C. Zhang, Y. Su, Y. Lian, P. Qi, Z. Deng, D. Zhang, S. Wang, X. Zhu, Y. Peng, *Appl. Catal. B.,* 2020, 262, 118144.

S4 Q. Chen, S. Li, H. Xu, G. Wang, Y. Qu, P. Zhu, D. Wang, *Chinese Journal of Catalysis.,* 2020, 41, 514–523.

S5 M. Xu, H. Wu, Y. Tang, G. Mao, G. Wang, L. Zhang, Q. Liu, *Microporous and Mesoporous Materials.,* 2020, 309, 110539.

S6 X. Jin, C. Lv, X. Zhou, H. Xie, S. Sun, Y. Liu, Q. Meng, G. Chen, *Nano Energy.,* 2019, 64, 103955.

S7 Y. Bai, P. Yang, L. Wang, B. Yang, H. Xie, Y. Zhou, L. Ye, *Chem. Eng. J.,* 2019, 360, 473–482.

S8 X. Kong, W.Q. Lee, A. R. Mohamed, S-P. Chai, *Chem. Eng. J.,* 2019, 372, 1183–1193.

S9 J. Hu, J. Ding, Q. Zhong, *Journal of Colloid and Interface Science.,* 2020, 560, 857–865.

S10 S. Wan, M. Ou, Q. Zhong, X. Wang, *Chem. Eng. J.,* 2019, 358, 1287–1295.